Int. J. Solids Structures Vol. 19, No. 4, pp. 305–314, 1983
Printed in Great Britain.

0020-7683/83/040305-10$03.00/0
Pergamon Press Ltd.

STRESS WAVE PROPAGATION IN RODS OF ELASTIC-VISCOPLASTIC MATERIAL†

S. R. BODNER
Faculty of Mechanical Engineering, Technion-Israel Institute of Technology, Haifa 32000, Israel

and

J. ABOUDI
Dept. of Solid Mechanics, Materials and Structures, Tel Aviv University, Tel Aviv, Israel

(*Received* 1 *April* 1982; *received for publication* 8 *July* 1982)

Abstract—A number of uniaxial stress wave propagation problems are solved based on the unified, multi-dimensional, elastic-viscoplastic constitutive equations of Bodner-Partom and a finite difference numerical procedure. Solutions are obtained for cases of a velocity imposed for a time period or indefinitely at the end of a semi-infinite bar, and for the condition of a finite bar subjected to a high velocity superimposed on an applied low velocity after a time interval. Work-hardening is taken to be isotropic for stress of constant sign, while an isochoric, anisotropic work-hardening formulation is employed for problems involving stresses of reversed sign due to unloading or reflections. The numerical exercises are based on constants for a strongly strain rate sensitive material, titanium, and the results indicate good qualitative agreement with a wide range of experimental observations.

INTRODUCTION

The study of plastic waves in solids has had an unusually controversial history considering that the geometry, loading circumstances, and the boundary and initial conditions could be precisely defined. It seems that one of the essential difficulties in analytical treatments is the modelling of the inelastic material properties and their subsequent use in the field equations. Certain response characteristics are sensitive to the details of the material characterization while others are insensitive to gross variations in the modelling, as discussed e.g. [1–3]. This variation of response characteristics has led to much of the controversy when analytical predictations based on particular material representations have been compared with experimental results. Another source of difficulty for the most studied case of longitudinal stress waves in long rods is the determination of the relative importance of transverse inertia and straining effects which are usually omitted in the conventional one dimension analyses. These could be of some significance near the impacted end and at early times, which are the circumstances when rate of straining effects are most influential. An extensive discussion on these points is included in the recent review article on elastic–plastic stress waves by Nicholas [4].

There have been developments in recent years in the formulation of constitutive equations which are more realistic representations of the actual physical behavior of materials than the conventional models. In addition, considerable advances have taken place in methods of numerical analyses and in computational capability which make solving highly nonlinear problems appreciably simpler. For these reasons, the problem of uniaxial wave propagation in rods of elastic–viscoplastic material deserves reexamination.

In this paper, the constitutive equations of Bodner–Partom for elastic–viscoplastic work-hardening materials [5, 6] are used for the material characterization. These do not require a specific yield criterion or loading–unloading conditions which make them particularly suitable for dynamic plasticity problems. The formulation is, therefore, different from that based on a strain rate dependent yield criterion such as that of Perzyna which was used in a recent study [7]. The ability of the equations of [5, 6] to represent and predict a wide range of dynamic material response characteristics has been demonstrated in a number of exercises [6, 8–10]. An isotropic work-hardening formulation was employed in most of these examples which was

†This research was sponsored in part by the Air Force Office of Scientific Research/AFSC under grant AFOSR-80-0214, through the European Office of Aerospace Research and Developmemt (EOARD), U.S. Air Force.

suitable for the given conditions. For wave propagation problems that involve unloading and reflected waves, an anisotropic hardening theory that would include the "Bauschinger effect" is required. In the present exercises, this is accomplished by a modified (isochoric) version of the anisotropic hardening theory of[11] which is identical to that of[12] for the one dimensional stress case.

It is noted that although only uniaxial stress and inertia terms are considered in the problem, the strains are three-dimensional and the multi-dimensional form of the constitutive equations is required. The small strain approximation is employed in these examples, but it seems possible to generalize the formulation to large strains without much difficulty.

Numerical examples are given for conditions of a velocity imposed for a time period or indefinitely at the end of a semi-infinite rod, and for the case of a finite rod subjected to a high velocity superimposed on a low velocity after a time interval. The numerical procedure is based on finite differences in which some new techniques enable rapid convergence of the results. The numerical results are compared to those of various experiments and to the predictions of the more classical theories.

FORMULATION OF GOVERNING EQUATIONS

We consider a thin rod for which the only non-zero stress σ_{11} is in the axial x_1 direction so that the equation of motion is

$$\rho\ddot{u}(x_1, t) = \sigma_{11,1} \tag{1}$$

where u is the axial particle displacement and ρ is the mass density. Inertia effects are assumed to occur only in the axial direction but transverse strains and strain rates are present. All the strains are taken to be functions of x_1 and constant in the transverse directions x_2 and x_3. On the basis of the strain-displacement gradient relation, $\epsilon_{11} = u_{,1}$ and separation of the total strain into elastic and inelastic components with Hooke's Law applying for the elastic strain, the equation of motion could be expressed as

$$\rho\ddot{u}(x_1, t) = E[u_{,11} - \epsilon^p_{11,1}] \tag{2}$$

where E is the Young's Modulus.

The elastic–viscoplastic constitutive equations with isotropic work hardening are those formulated by Bodner and Partom[5, 6] which are based on taking the elastic and plastic deformation rates (strain rates for small strains) to be additive and each non-zero at all stages of loading and unloading. Other essential assumptions of the theory are that the Prandtl–Reuss flow equation applies for the plastic strain rate,

$$\dot{\epsilon}^p_{ij} = \lambda s_{ij} \tag{3}$$

and that inelastic deformation is governed by a continuous relation between the second invariant of the plastic strain rate D_2^p, and the second invariant of the stress deviator J_2. That is $D_2^p = F(J_2, Z_k, T)$ where Z_k are internal state variables defining the inelastic state with respect to deformation, and T is the temperature. Squaring (3) and solving for λ, i.e.

$$\lambda = (D_2^p/J_2)^{1/2} \tag{4}$$

enables the total strain rates to be expressed as functions of the uniaxial stress $\sigma_{11} = \sigma$, stress rate $\dot{\sigma}$, and state variables which are incorporated in the λ term,

$$\dot{\epsilon}_{11} = (1/E)\dot{\sigma} + (2/3)\lambda\sigma \tag{5a}$$

$$\dot{\epsilon}_{22} = \dot{\epsilon}_{33} = (-\nu/E)\dot{\sigma} - (1/3)\lambda\sigma. \tag{5b}$$

A particular form for D_2^p suggested in [5, 6] is

$$D_2^p = D_0^2 \exp[-(Z^2/3J_2)^n(n + 1/n)] \tag{6}$$

where D_0^2 is the limiting value of D_2^P, n is related to the steepness of the $D_2^P - J_2$ curve and therefore controls strain rate sensitivity, and Z is a scalar internal state variable which represents the overall resistance to plastic flow, i.e. it is a history dependent work-hardening parameter. The evolution equation for Z is based on plastic work W_p as the controlling factor in hardening, so that

$$\dot{Z} = \left(\frac{dZ}{dW_p}\right)\left(\frac{dW_p}{dt}\right) \tag{7}$$

where $\dot{W}_p = \sigma\dot{\epsilon}_{11}^P$ in this case. A form chosen for dZ/dW_p in the previous work is

$$\frac{dZ}{dW_p} = (m/Z_0)(Z_1 - Z). \tag{8}$$

On the basis of (8), eqn (7) could be integrated to give

$$Z = Z_1 - (Z_1 - Z_0)\exp(-mW_p/Z_0) \tag{9}$$

where Z_0 is the constant of integration, i.e. the value of Z for $W_p = 0$.

For stress waves that undergo unloading and reflections with consequent reloading in the opposite direction, it is appropriate to include anisotropic (directional) hardening, the "Bauschinger Effect", into the material characterization. A multiaxial anisotropic hardening law was formulated in [11] in conjunction with an anisotropic form of the Prandtl–Reuss flow law as a generalization of the constitutive equations. However, plastic incompressibility was not imposed which could lead to physically unrealistic plastic volume changes and possible inconsistancy with Drucker's Postulate under special loading conditions[14]. Despite this, the stress and strain fields obtained in [13] for various problems using the compressible anisotropic formulation of [11] appear to be essentially correct.

A method of resolving the difficulty is to maintain the anisotropic hardening law proposed in [11], which has a number of desirable features and appears to be reasonably realistic, and to enforce incompressibility of plastic flow as an additional condition. Procedures for doing this are described in [14], and lead to consistency of the anisotropic hardening formulation with stability considerations.

In the case of uniaxial stress, imposition of plastic incompressibility results in incremental isotropic of the flow law, i.e. the flow law is necessarily isotropic at each time increment even though hardening is anisotropic. That is, eqn (3) is applicable where the coefficient λ depends on an effective hardening variable which is a scalar function of the components of a general hardening tensor. The definition of the effective hardening variable proposed in [14] reduces to the procedure for anisotropic hardening described in [12] for uniaxial stress of changing sign. That method, which involves uniaxial hardening components in tension and compression, was used in the present calculations in examples exhibiting reversed stresses due to unloading and reflections. An additional material constant, q, appears in the anisotropic hardening formulation which is the proportion of the hardening increment that is isotropic while the remainder is anisotropic (directional). It is noted that the incremental form of the evolution equation, (8), must be used for these calculations where Z is the current value of the applicable hardening variable depending on the sign of the stress.

NUMERICAL TREATMENT

The governing equations have been solved numerically by a finite difference procedure by dividing the bar into equal sub-intervals of size Δx_1, and introducing a time increment Δt. The procedure is described in [13] for a 2-dimensional dynamic problem and it is summarized here for the present uniaxial stress situation.

The numerical solution can be divided into three parts. In the first part, the displacements at interior points of the bar are computed by integrating the equation of motion (2). In the second part, the plastic strains and plastic work are determined, while the displacements at the end points of the bar are computed in the third part.

Part 1

The displacement $u(x_1, t)$ at the interior points of the bar is governed by the equation of motion (2). This is integrated, giving the second order approximation

$$u(x_1, t+\Delta t) = 2(1-k^2)u(x_1, t) - u(x_1, t-\Delta t) + k^2[u(x_1+\Delta x_1, t) + u(x_1-\Delta x_1, t)]$$

$$-(1/2)k^2\Delta x_1[\epsilon_{11}^p(x_1+\Delta x_1, t) - \epsilon_{11}^p(x_1-\Delta x_1, t)] \tag{10}$$

where

$$k^2 = \frac{E}{\rho}\left(\frac{\Delta t}{\Delta x}\right)^2.$$

According to (10), it is possible to compute the displacement u at an internal point at time $t+\Delta t$ provided its value at the previous and present time steps, $t-\Delta t$, and t respectively, as well as the values of the plastic strain ϵ_{11}^p at time t, are known throughout the bar.

Part 2

The finite difference procedure for this part is identical to that described in [13]. It is noted that eqn (25) of [13], on the basis of [14], reduces for the present uniaxial case to

$$Z^{\pm}(x_1, t) \cong Z^{\pm}(x_1, t-\Delta t) + q\Delta Z(x_1, t) \pm (1-q)\Delta Z(x_1, t)[\sigma_{11}/|\sigma_{11}|] \tag{11}$$

where ΔZ is the increment of Z in the time change Δt, and Z^+ and Z^- are the hardening variables in the directions of the positive and negative stress axes, i.e. tension and compression.

A misprint occurred in eqn (27) of [13]; it should read for this case

$$\dot{Z}(x_1, t) \cong (m/Z_0)[Z_1 - Z(x_1, t)]\dot{W}_p(x_1, t-\Delta t). \tag{12}$$

Part 3

The boundary values of the displacement at $x_1 = 0$ are determined from the velocity input $\dot{u}(x_1 = 0) = V_i(t)$ giving

$$u(x_1 = 0, t) = \int_0^t V_i(\zeta)\,\mathrm{d}\zeta \tag{13}$$

If the applied loading were of the stress type, $\sigma_{11} = p(t)$ at $x_1 = 0$, then the condition on the end displacement would be

$$u(x_1 = 0, t) = u(\Delta x_1, t) - \Delta x_1\{[p(t)/E] + \epsilon_{11}^p(x_1 = 0, t)\}. \tag{14}$$

For a rigidly clamped end,

$$u(x = H, t) = 0. \tag{15}$$

APPLICATIONS

A number of examples were calculated to obtain the stress, strain and displacement fields (x_1, t) of bars subjected to an imposed velocity at one end. The computations were based on commercially pure titanium as the bar material using the same elastic and plastic material constants as in[6, 13]: E(elastic) = 1.18×10^5 MPa, μ(elastic) = 0.44×10^5 MPa, $\rho = 4.87$ gm/cm^3, $Z_0 = 1150$ MPa, $Z_1 = 1400$ MPa, $D_0 = 10^4\,\mathrm{sec}^{-1}$, $n = 1$ and $m = 100$, and from [12], $q = 0.05$. Commercially pure titanium is strongly strain rate sensitive[6, 8], and a change in strain rate from $3 \times 10^{-3}\,\mathrm{sec}^{-1}$ to $3\,\mathrm{sec}^{-1}$ would cause an increase of the flow stress of about 35%, Fig. 1, while higher rates would result in larger factors. Stress–strain curves computed from the above constants, Fig. 1, indicate the absence of a reference "static" curve which is fundamental to the

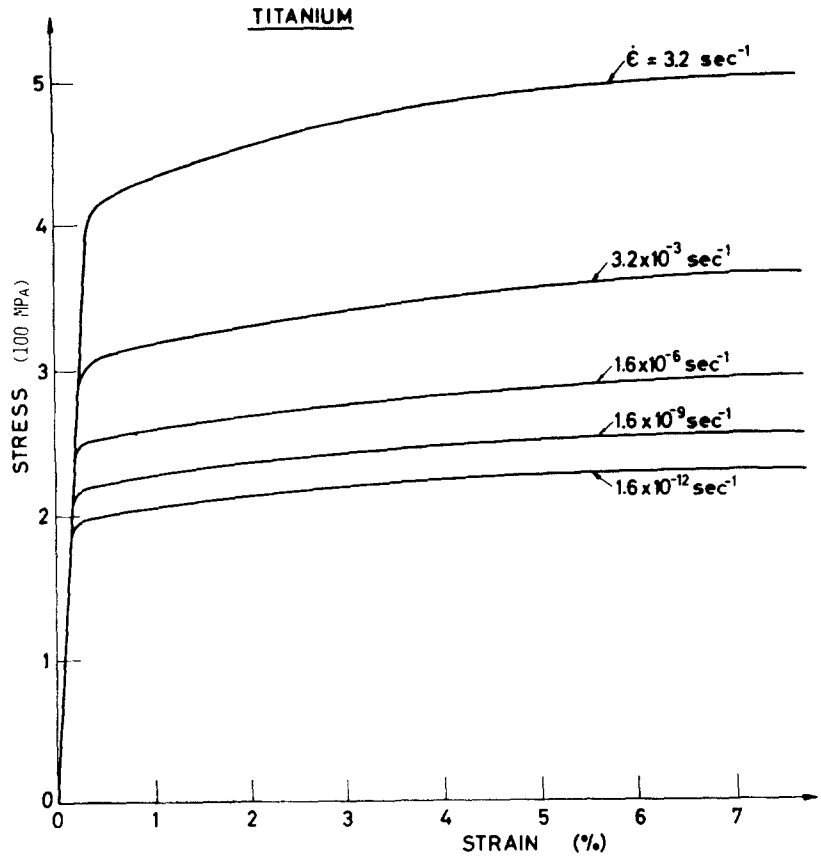

Fig. 1. Calculated stress-strain curves for titanium at different applied strain rates.

formulation, although the relative rate sensitivity at the low rates is appreciably smaller than at the high rates. In the wave propagation examples, the plastic strain rates near the struck end at early times after impact (about 50 μs) were of the order of $10^3\ sec^{-1}$.

The numerical examples were for cases of semi-infinite and finite bars subjected to a constant velocity at one end which was maintained either indefinitely or for a specific time period. In addition, the condition of a high velocity superimposed on a low velocity at the end of a finite bar was run. A particular length of finite bar was used in the examples, namely $H = (c_1 D_0^{-1}/5)$ which for titanium corresponds to $H = 0.122$ m. In this paper, c_1 denotes the velocity of dilatational waves, $c_1 = [\mu(4\mu - E)/(3\mu - E)\rho]^{1/2}$, and c_0 is the bar velocity, $c_0 = (E/\rho)^{1/2}$. For titanium, $c_1 = 6100$ m/s and $c_0 = 5000$ m/s. For most of the numerical examples, the spatial increments were $\Delta x_1/H = 0.01$ and the time steps 0.18 μs, but these were decreased by a factor of 5 in some cases (Figs. 2 and 3). A typical computation on an IBM 370/168 of all the response quantities for an elapsed time of 150 μs required about 10 min. computation time for the semi-infinite bar and about 3 min. for the finite bar. It should be mentioned that preliminary results using a much courser grid were communicated to Nicholas and reported in [4].

DISCUSSION OF RESULTS

Graphs illustrating results of the numerical exercises are shown in Figs. 2–6. Figures 2 and 3 show the stress and strain response for a semi-infinite rod subjected to a suddenly applied and maintained velocity V_i at the free end $x_1 = 0$. Some of the response features shown in Fig. 2, which gives spatial distributions at different times, are the propagation of the wave front at the elastic bar velocity, c_0, the appearance of an apparent "yield stress", i.e. the amplitude of the wave front, which decays with time, and the tendency of the stress and plastic strain levels to form a "plateau", i.e. to be almost constant, near the struck end despite the strong rate sensitivity of the material. The oscillations in the stress-distance plot are due to the finite

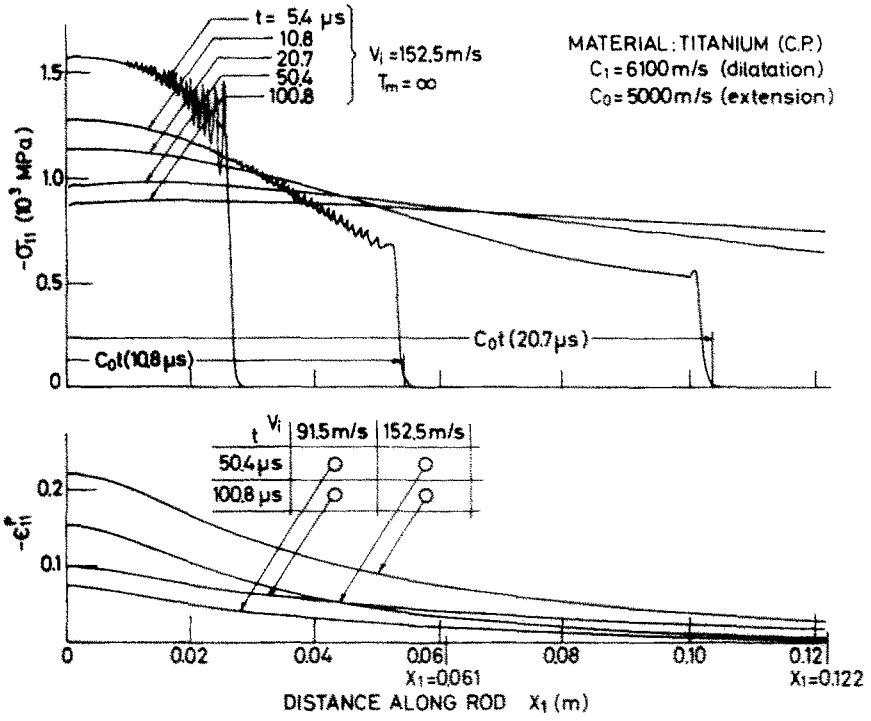

Fig. 2. Stress and plastic-strain distribution in a semi-infinite bar subjected to constant velocity impact at end.

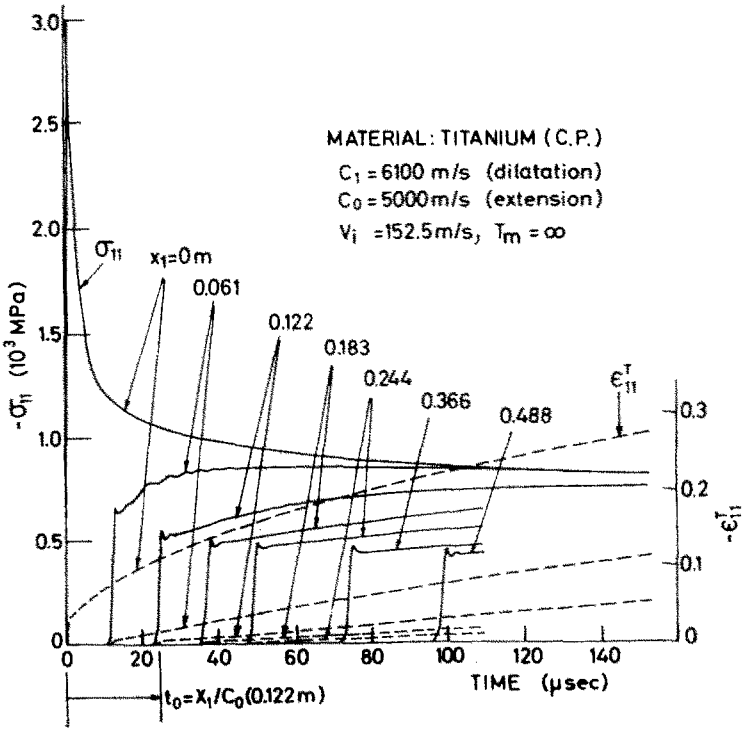

Fig. 3. Stress and total-strain histories in a semi-infinite bar subjected to constant velocity impact at end.

difference numerical solution and are not a consequence of radial inertia effects which are absent in the present formulation. These could have been eliminated by a numerical procedure, but were maintained to ensure that the basic response information is maintained.

The stress variations with time and distance near the struck end show some interesting characteristics. At the end $x_1 = 0$, the immediate response to the applied velocity is fully elastic, Fig. 3, and the stress peak corresponds exactly to the elastic relation $\sigma = \rho c_0 V_i$. This stress decays rapidly with time and reaches a third of the original value in 30 μs. The wave front amplitude also decays with distance and reaches a value of 410 MPa after 50 cm of travel (100 μs). This "yield stress" corresponds to a strain rate of about $3\,\text{sec}^{-1}$ which is slow compared to the initial plastic strain rates which are of the order of $10^3\,\text{sec}^{-1}$. It is still 35% higher than the "quasi-static" yield stress, i.e. that corresponding to a strain rate of about $10^{-3}\,\text{sec}^{-1}$, Fig. 1.

These computed results tend to be in qualitative agreement with experimental observations although direct comparison with identical specimen materials and experimental conditions is not available. Impact tests on rods of a similar, but not identical, titanium are reported by Hsu and Clifton in [15], together with a rate dependent analysis for the test conditions.

Plateaus of constant stress and plastic strain near the struck end of impacted rods are generally observed, e.g.[1], and have in the past been the catalyst for arguments on the rate independence of specimen materials. It is interesting to note that these plateaus computed from a rate dependent formulation exist even for short times after impact. The presence of a high elastic stress peak at the struck end, as shown in Fig. 3, has been observed experimentally by Bell[16] and noted by Cristescu[17]. Detailed examination of the strain-time results show that the propagation velocity of equal strain levels is almost constant at small strains ($\sim 1\%$), but deviates from constant at high strains. Similar results were obtained both experimentally and analytically for titanium in [15]. A constant wave velocity is predicted by the rate independent plastic wave theory and has been observed experimentally by Bell[18] for relatively rate insensitive materials such as aluminum and copper. Another point of departure from the rate independent theory and the observations of Bell[19] is the absence of a strain maximum on the strain-time plot, Fig. 3. However, results corresponding to Fig. 3 have been obtained both experimentally and analytically for titanium in [15].

For long times after impact, the maximum stress that propagates at the elastic bar velocity is generally observed to correspond to the "static-yield stress", e.g.[1]. However, for a strongly rate dependent material such as titanium, relaxation to the "quasi-static" yield stress is seen in Figs. 2 and 3 and in the results of [15] to be relatively slow. "Yield stresses" that are 30–40% above the quasi-static value are obtained for times 100–200 μs after impact. The tendency of the results of a rate dependent formulation to approach the "quasi-static" response with increasing time has been noted by others and is discussed in [4]. A reference "static" stress–strain curve is not included in the reference constitutive equations, but rate dependence in the low rate range is relatively weak. Once the plastic strain rates drop to the low range, decay of the stress front is fairly slow with time and distance.

Another numerical exercise was the case of a finite rod which is fixed at one end and subjected to a low velocity at the free end for a time period after which the velocity is suddenly increased to a high value. The initial low velocity, $V_0 = 1.22 \times 10^{-4}$ m/s, does not introduce inertial effects and creates a uniform strain rate of $10^{-3}\,\text{sec}^{-1}$ over the bar length. At a total strain of 0.03, the high velocity, $V_i = 61.0$ m/s, is suddenly imposed which leads to elastic–plastic stress waves. Stress and strain response to the high velocity are shown in Figs. 4 and 5 as functions of distance and time respectively. One of the features of the results is that the wave front travels at the elastic bar velocity which is expected for a rate dependent material. This wave front exhibits a finite amplitude which decays with time and distance. In fact, the overall response results for a velocity applied to a prestrained rod, Figs. 4 and 5, are similar to those of a high intensity velocity on an unstrained rod, Figs. 2 and 3, with somewhat more rapid decay of the wave front. The results also appear to be similar to those obtained experimentally for corresponding conditions such as those reported in [19].

An unusual result in Fig. 5 is the increase in the wave front amplitude at the fixed end, but this is due to the doubling of the elastic stress component at that station. The elastic front reaches the end of the rod in 24.4 μs. By the time the elastic wave front returns to the free end

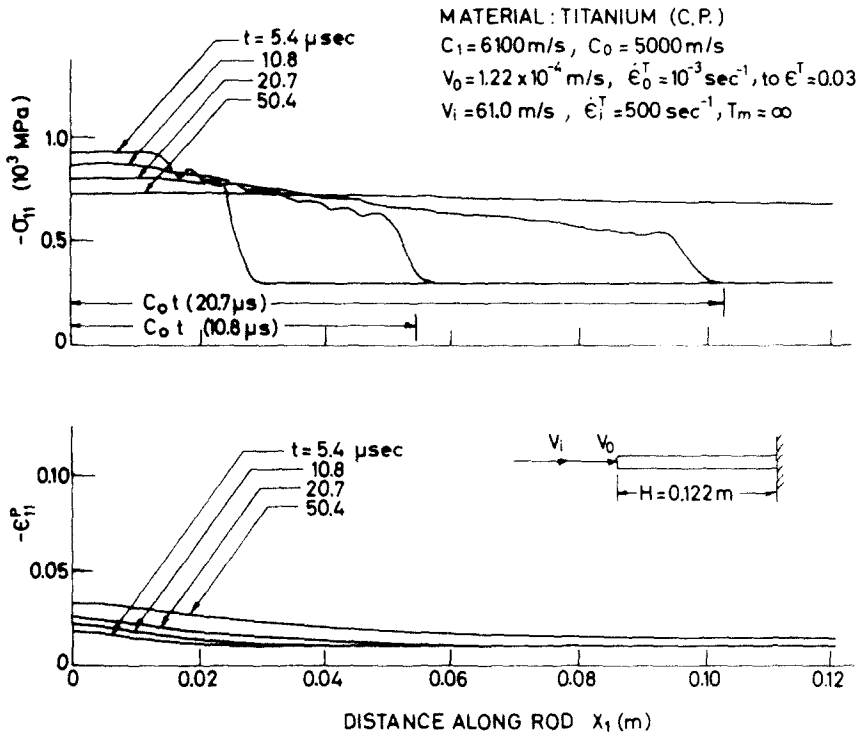

Fig. 4. Stress and plastic-strain distribution in a finite bar subjected to a constant high velocity impact at end superimposed on a low velocity after a time interval.

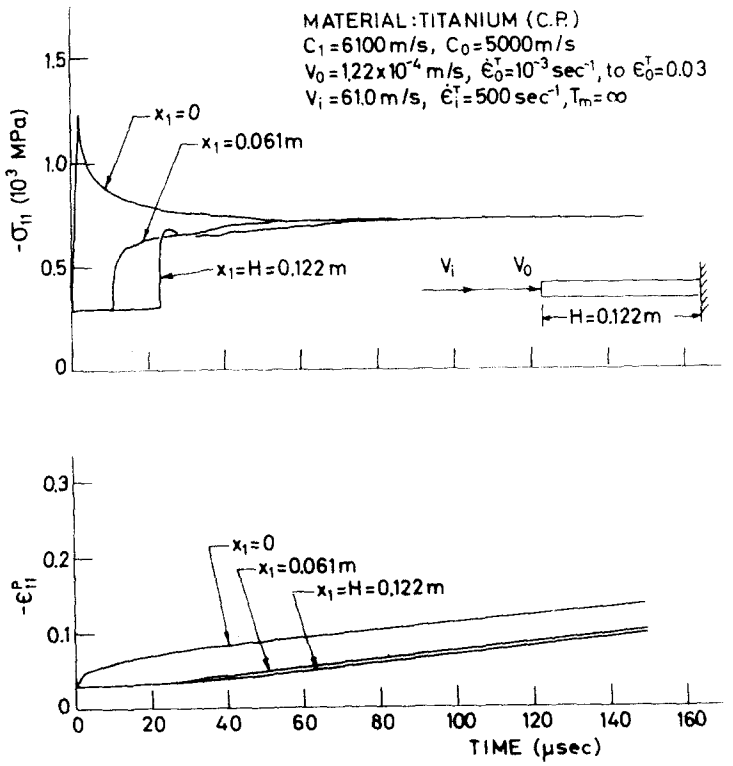

Fig. 5. Stress and total-strain histories in a finite bar subjected to a constant velocity impact at end superimposed on a low velocity after a time interval.

of the rod, wave effects are almost eliminated and the rod extends at an almost uniform strain rate of 500 sec^{-1} due to the applied velocity. An elastic wave of diminishing amplitude would continue to propagate along the rod for some time. Under steady state conditions, the situation would correspond to a quasi-static test in which a specimen is subjected to a sudden increase in strain rate. After a rapid jump in stress level, the flow stress is governed by the applied strain rate and the amount of work hardening (plastic work).

A set of exercises was run for cases of a velocity V_i applied to the end of a semi-infinite rod for a prescribed time period T_m, and a typical result is shown in Fig. 6. The stress and strain response is identical to that given in Figs. 2 and 3 until the removal of the applied velocity which for Fig. 6 occurred at $T_m = 40\,\mu s$. Unloading then sets in with resulting stress waves of reversed sign. In these computations, the anisotropic hardening formulation was employed as described previously with the material constant $q = 0.05$ as in [12]. In Fig. 6, the oscillations upon unloading are due to numerical effects.

It is noted in Fig. 6 that the initial unloading response at the struck end is almost completely elastic with a resulting high stress in the opposite direction. The high stress levels due to both loading and unloading decay with time and distance and the stress pulse assumes a fairly stable form after some distance along the rod. The computed wave form at the station $x_1 = 12.2\,cm$ from the struck end could be compared to that obtained experimentally in [20] for elastic-plastic pulse propagation in long rods of aluminum. Fig. 12 of [20] gives the experimental strain-time response at a remote station from the impacted end, from which a stress-time curve similar to Fig. 6 could be deduced based on the strain rate independent plastic wave theory. A Bauschinger effect on the reversed stress was evident from the experimental results of [20]. The present rate dependent formulation includes a Bauschinger effect (anisotropic hardening) and predicts stress-time and strain-time relations at stations removed from the impact end, Fig. 6, that appear similar in form to those obtained experimentally in [20] for a rate insensitive material but with flow stress levels raised above the "quasi-static" values.

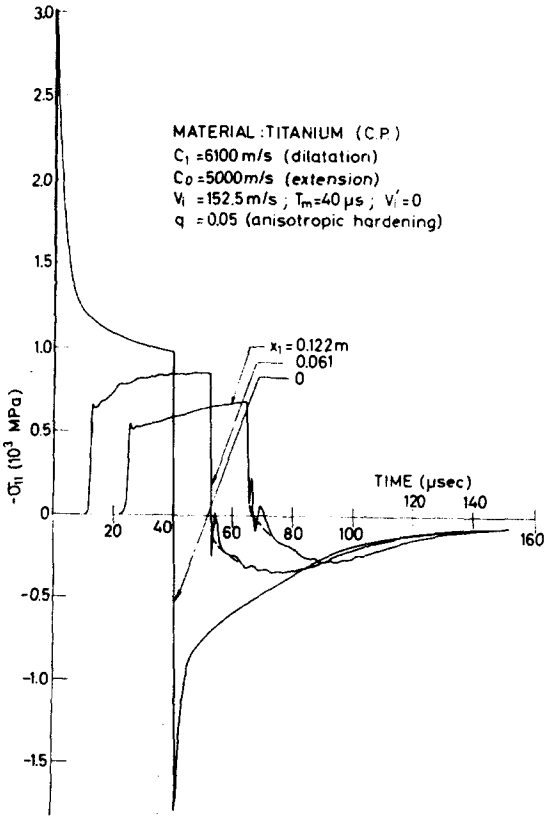

Fig. 6. Stress history in a semi-infinite bar subjected to a constant velocity impact at end for a prescribed time period. $T_m = 40\,\mu s$.

CONCLUSIONS

A set of constitutive equations that serves to realistically represent the strain-rate dependent and work-hardening inelastic properties of metals has been used to solve a variety of uniaxial wave propagation problems by the finite difference method. Numerical exercises for a strongly rate-dependent material, titanium, show response characteristics which are consistent with a number of experimental observations. These include the appearance of a "plateau" of almost constant stress and plastic strain with distance near the impacted end of long rods, the instantaneous elastic response at the struck end which rapidly decays with time, the attenuation of the initially high amplitude of the elastic stress front to a "slow strain rate" value, the inital elastic response of plastically deformed rods to suddenly applied superimposed loading, and the tendency of the response to pulse loading to approach that of the rate independent plastic wave theory at long times after initial impact. Strain-time profiles do not show a plateau of uniform strain which would be indicated by the rate-independent theory, and the propagation velocity of a high strain ($> 1\%$) is not constant. These results demonstrate the importance of the use of rate-dependent constitutive equations for such cases even though certain phenomena are predicted by the rate-independent theory. In addition, it is shown that anisotropic work-hardening (the Bauschinger Effect) should be considered for the pulse loading condition.

REFERENCES

1. H. Kolsky and L. S. Douch, Experimental studies in plastic wave propagation. *J. Mech. Phys. Solids.* **10**. 195–233 (1962).
2. E. A. Ripperger and H. Watson, Jr., The relationship between the constitutive equation and one-dimensional wave propagation. *Mechanical Behavior of Materials under Dynamic Loads* (U.S. Lindholm Ed.), pp. 294–313. Springer-Verlag, New York (1968).
3. T. Nicholas, On the determination of constitutive equations from plastic wave propagation phenomena. U.S. Air Force Materials Lab., Tech. Rep. AFML-TR-73-73 (1973).
4. T. Nicholas, Elastic-plastic stress waves. *Impact Dynamics*, (Edited by J. A. Zukas, *et al.*), pp. 95–153. Wiley, New York (1982).
5. S. R. Bodner and Y. Partom, Dynamic inelastic properties of materials—representation of time dependent characteristics of metals. *Proc. ICAS Conf.*, Amsterdam, Paper 72-28 (1972).
6. S. R. Bodner and Y. Partom, Constitutive equations for elastic-viscoplastic strain-hardening materials. *J. Appl. Mech., Trans. ASME* **42**, 385–389 (1975).
7. C. T. Chon and G. J. Weng, Impact of a finite elastic-viscoplastic bar. *Int. J. Non-linear Mech.* **15**, 195–209 (1980).
8. A. Sperling and Y. Partom, Numerical analysis of large elastic-plastic deformation of beams due to dynamic loading. *Int. J. Solids Structures* **13** 865–876 (1977).
9. S. R. Bodner and A. Merzer, Viscoplastic constitutive equations for copper with strain rate history and temperature effects. *J. Engng Mater. Tech., Trans. ASME* **100**, 388–394 (1978).
10. S. R. Bodner, Representation of time dependent mechanical behavior of René 95 by constitutive equations, U.S. Air Force Materials Lab., Techn. Rep. AFML-TR-79-4116 (1979).
11. D. C. Stouffer and S. R. Bodner, A constitutive model for the deformation induced anisotropic plastic flow of metals. *Int. J. Engng Sci.* **17**, 757–764 (1979).
12. S. R. Bodner, I. Partom and Y. Partom, Uniaxial cyclic loading of elastic-viscoplastic materials. *J. Appl. Mech. Trans. ASME* **46**, 805–810 (1979).
13. J. Aboudi and S. R. Bodner, Dynamic response of a slab of elastic-viscoplastic material that exhibits induced plastic anisotropy. *Int. J. Engng Sci.* **18**, 801–813 (1980).
14. S. R. Bodner and D. C. Stouffer, Comments on anisotropic plastic flow and incompressibility. *Int. J. Engng Sci.* (in press).
15. J. C. C. Hsu and R. J. Clifton, Plastic waves in a rate sensitive material—I. Waves of uniaxial stress. *J. Mech. Phys. Solids* **22**, 233–253 (1974).
16. J. F. Bell, The initiation of finite amplitude waves in annealed metals. *Stress Waves in Anelastic Solids*, (H. Kolsky and W. Prager (Eds), pp. 166–182. Springer-Verlag, New York (1964).
17. N. Cristescu, *Dynamic Plasticity*, p. 172. North Holland, Amsterdam (1967).
18. J. F. Bell, *The Physics of Large Deformation of Crystalline Solids*. Springer-Verlag, New York (1968).
19. T. V. Santosham and H. Ramsey, Small plastic strain wave propagation in prestressed soft copper rods. *Int. J. Mech. Sci.* **12**, 447–457 (1970).
20. S. R. Bodner and R. J. Clifton, An experimental investigation of elastic-plastic pulse propagation in aluminum rods. *J. Appl. Mech., Trans. ASME* **34**, 91–99 (1967).